Correlation Among Powder Morphology, Compactability, and Mechanical Properties of Consolidated Nascent UHMWPE

G. H. Michler,[1] V. Seydewitz,[1] M. Buschnakowski,[1] L. P. Myasnikowa,[2] E. M. Ivan'kova,[2] V. A. Marikhin,[2] Y. M. Boiko,[2] S. Goerlitz[1]

[1]*Institute of Physics, Martin-Luther-University Halle-Wittenberg, Halle/S. D-06099, Germany*
[2]*A. F. Ioffe Physical-Technical Institute, Russian Academy of Sciences, St. Petersburg 194021, Russia*

Received 11 September 2009; accepted 27 February 2010
DOI 10.1002/app.32346
Published online 26 May 2010 in Wiley InterScience (www.interscience.wiley.com).

ABSTRACT: The influence of the catalytic system and synthesis conditions on the reactor powder morphology and the molecular packing in the nascent UHMWPE is studied with the help of various electron microscopic methods. The potentiality of different morphologies for producing strong consolidated material by sintering at temperature lower than the melting temperature is considered. It is shown that the small catalytic particles of colloidal sizes (reactor powders of M-series) produce homogeneous broccoli type morphology consisting of small nodules with the sizes less than 0.2–0.5 μm, which in turn, comprise crystalline domains and disordered regions. Comparison analysis of transmission electron microscopic data with the DSC and NMR results enabled to conclude that the disordered regions are predominantly comprised of tie molecules with low degree of coiling, taut tie molecules, and a number of tight folds. This type of morphology best fits for compaction and sintering. Reactor powder morphology arising upon synthesis lab-scale and commercial UHMWPE on supported catalysts is not so homogeneous, and consists of miscellaneous morphological units, such as spirals, flakes, secondary fibrils, interconnecting the subparticles, large and small lamellae in depending of the catalyst system. The density of disordered regions in these reactor powders is less than that in the particles of M-series. The tensile strength of the samples obtained by sintering of the M-powders is higher than the strength of the other ones by a factor 2.5, which makes them good precursors for orientation drawing. J Appl Polym Sci 118: 866–875, 2010

Key words: polyethylene; morphology; processing; electron microscopy

INTRODUCTION

Ultra-high molecular weight polyethylene (UHMWPE) with molecular weights of some 10^6 (g/mol) is a large tonnage polymer due to its unique properties, such as high mechanical properties, low friction, high abrasive, and chemical resistance etc., and wide practical applications from bullet-proof jackets and armours, fishing lines, ropes, and sporting-goods up to medical artificial joints. However, UHMWPE cannot be produced by the conventional methods (extrusion, injection molding…) because of the very high viscosity of its melt.

For production of high-strength, high-modulus UHMWPE fibers, a special gel-technology was developed (solving the reactor powder and subsequently drawing a gel formed from the cooled solution[1]). However, the use of a large volume of organic solvent in this process makes gel-technology environmentally nonfriendly and expensive. In the past, some of the UHMWPE reactor powders turned out to be highly compactable and drawable.[2] An opportunity to realize a "dry" route to high-performance fibres directly from reactor powders without melting or dissolving the material ("never-processed" PE) became then very challengeable. It was materialized on a lab-scale in a number of laboratories throughout the world, and samples with mechanical characteristics comparable to those reached by gel-technology were obtained.[3–5] The most stiff and strong UHMWPE tapes ($\sigma = 3.4$ GPa, $E = 123$ GPa) were produced at lab-scale by solution-free method from reactor powder, which was synthesized on vanadium catalyst system at very low temperature (−18 °C).[2] This temperature is not obviously fitted for industrial production. The value of Young's modulus of the tapes produced on lab-scale from UHMWPE reactor powders synthesized on various Ziegler-Natta-type catalytic systems at higher temperatures (40–60°C) was almost the same but tensile strength was lower ($\sigma = 1.5$–1.6 GPa).[4,5]

Correspondence to: G. H. Michler (goerg.michler@physik.uni-halle.de).

Contract grant sponsors: Deutsche Forschungsgemeinschaft.

The attempt to commercialize "dry" processing was undertaken in 1994 by Nippon Oil Company, which then licensed the solid-state technology for fibre production to USA to Synthetic Industries (SI), who worked with Integrated Textile Systems (ITS). This product is produced under the Tensylon trademark.[6] It is worthy to note that the fibre produced via solution-free technology have lower creep than gel-spun fibres. They are already utilized as advanced fibre composites in ballistic products, as well as in a wide variety of applications, where low cost, low creep, colour, UV stability, or exceptional abrasive resistance is required. The mechanical characteristics, however, are not very good (σ = 1.9 GPa, E = 120 GPa), as compared to those of gel-spun fibres, for instance, to Dyneema SK 76 from DSM (The Netherlands) (σ = 3.6 GPa, E = 116 GPa[7]). Thus, there is still a large gap between gel-spinning and solution-free technology.

The majority of authors consider low density of entanglements as the main factor controlling high drawability of the nascent UHMWPE.[5,8–10] However, not all UHMWPE powders with low density of entanglements demonstrate high drawability. Before drawing, the nascent particles should be compacted in a solid precursor strong enough to take an orientation stress and not to be untimely broken down along the intergrain boundaries. If the intergrain boundaries would not be well "healed" by the cohesive bonds, the potentiality of the nascent material could not be materialized.

The mechanism of cohesive bonds generating between the particles is investigated to a great extent.[11–13] At the same time, no unique criteria have been formulated for selecting the appropriate materials for "dry" technology despite a large body of publications in this field.[14–16] In spite of the fact that solution-free process was recently commercialized, and UHMWPE tapes under Tensylon trademark are produced,[6] the continued interest to searching for parameters controlling the ability of nascent particles to coalesce and to better understanding the influence of reactor powder morphology on the properties of a precursor for further drawing is maintained, because Tensylon characteristics are not so impressive.

As mentioned one of the key problems in searching for a proper route to enhance mechanical properties of UHMWPE tapes produced by solution-free technology is to clarify the influence of catalyst system and synthesis parameters on reactor powder processability, as well as finding optimum conditions for producing a mechanically coherent strong film by precompaction and sintering.

In this work, the electron microscopic data obtained for the same reactor powders described in[17] will be considered in more detail and matched with the mechanical properties of compacted and sintered tapes produced in different conditions. Optimum time–temperature–pressure conditions are to find for producing a strong precursor for further drawing.

One should emphasize that there are not so many publications[18,19] related to investigation of reactor powder fine structure using transmission electron microscopy because of complicate preparation work needed and high probability obtaining artefacts. Up to now, it was the first unique case to compare TEM investigations of very different reactor powders synthesized on different catalytic systems to study the influence of catalyst and synthesis parameters on reactor powder fine structure.[17]

To make this study more sensible, we investigated UHMWPE reactor powders, which were specially synthesized, compared with commercial reactor powders. It is worthy to note that there is another challenge for nascent UHMWPE polymer processing for producing polymer parts for hip and knee prosthesis. There are, however, requirements to the properties of compacted/sintered UHMWPE parts for artificial joints, differing from those to precursor for high performance fibres. These are high abrasive resistance, high impact strength, very smooth surface, high irradiation resistance, high thermal stability (because of necessity to be exposed to high temperature treatment for sterilization, etc.).

EXPERIMENTAL

Materials

UHMWPE reactor powders, which were synthesized at the Institute of Physico-Organic Chemistry of the National Academy of Sciences of Republic Belorussia, Minsk, and at "Plastpolymer", St. Petersburg, Russia, in desirable conditions, were studied. These were:

1. Reactor powders (RP) synthesized on one and the same catalytic system (highly active Ti/Cl catalytic system modified by Mg-organic compound), but at various temperatures (18, 30, 50, and 60°C, respectively: M-series)
2. RP synthesized at one and the same temperature (71°C), but at different catalytic systems ($TiCl_4$ and $TiCl_4{\cdot}Al_2O_3$-SiO_2: B568 and B570, correspondingly);
3. RP synthesized at 60°C but on catalysts of various shape (colloidal size of catalytic particles (M60) or a supported catalyst ($TiCl_3{\cdot}0.3AlCl_3{\cdot}MgCl_2$: B565).

Synthesis details and characteristics of the reactor powders are given in.[17] For comparison, several commercial reactor powders were used (e.g., Stamylan from DSM).

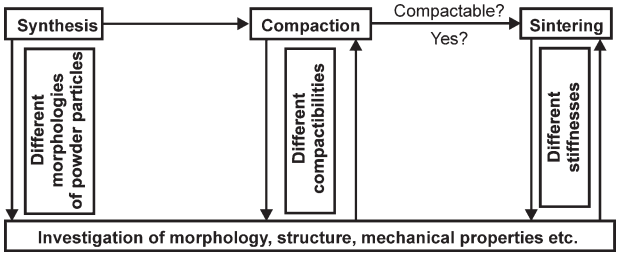

Figure 1 Schematic overview on the working steps.

Compaction/sintering of the powders

The reactor powders were compacted at room temperature under pressure. The optimum pressure of 95 MPa was chosen after comparative studies of mechanical characteristics of the samples compacted at various pressures (between 50 and 150 MPa for 5 to 10 min). The compaction is necessary to bring the nascent particles into "intimate" contact and eliminate air in between the particles at the great extent.

Second stage was sintering of a precompacted powder, which was carried out at the same pressure (95 MPa) and at the temperature lower than the melting point, i.e., it was annealing at the pressure. Annealing temperature (125°C) was chosen on the base of DSC data (the temperature had not to exceed the onset of melting). Annealing time varied in the range from 30 to 120 min.

Investigation of morphology

The reactor powder morphology and that of consolidated material was investigated using SEM and TEM techniques.[20]

Scanning electron microscopy

For SEM investigation the particles of nascent UHMWPE powders, compacted and precompacted/sintered tapes were adhered to conducting tapes on a sample holder, coated with a layer of gold 10–15-nm thick by sputtering and studied in a JEOL 6300 scanning electron microscope.

Transmission electron microscopy

For TEM observations a JEM 2010 electron microscope was used operating at 200 kV. The powders were stained by RuO_4 vapor, embedded in epoxy resin and stained by RuO_4 again. The consolidated samples were merely stained by RuO_4. This chemical treatment enhances the contrast between amorphous and crystalline parts of UHMWPE, and, additionally, hardens the material, enabling preparation of ultrathin sections using an ultramicrotome at room temperature. The stained samples were cut into thin sections of 80 nm thickness using a Leica Ultracut UCT microtome with a diamond knife (DIATOME).

Determination of mechanical properties

Mechanical properties of compacted and precompacted sintered pads have been determined using Minimat Microtensile Tester (Polymer Laboratories, Loughborough, UK). The compacted samples of about 150 μm thick and sintered tapes of 100 μm were cut to the narrow strips of 2 mm wide (length was 20 mm), and stress–strain curves were recorded at room temperature. The cross head displacement rate was 5.5 mm/min.

An overview on all the practical steps of the work is sketched in Figure 1.

RESULTS

Structure of the powder particles

Using SEM it was revealed that the different nascent particles of the lab-scale reactor powders have irregular shape and broad size distribution, whereas those of commercial powders are predominantly of spherical shape with a narrow size distribution.

Characteristic morphologies are shown in Figure 2. The individual particles of the powders have a complicate hierarchical structure comprising of large and small subparticles (nodules) (A), spiral-shaped worms and ribbons composed from flakes (B), or combination of nodules and fibrillar units (C). Concerning shape of powder particles, the shape and size of subparticles, their porosity and interconnection, three different types are classified:

- broccoli-like
- worm-like
- cob-web

SEM study only gives an appearance of different morphological units in the virgin polymers.

Details of the inner structure of powder particles have been revealed by TEM inspection of selectively stained ultrathin sections of the particles. TEM images are given in Figures 3, 5, 6. Characteristic morphological units of the different powder particles revealed from SEM and TEM data are summarized in Table I.

The morphological units resolved in a section of M30 nascent particle stained by ruthenium tetroxide seem like small light beads (Fig. 3). Somewhere they are disposed very close to each other and look like a short fibril. Obviously these nonstained beads are the crystalline domains. The question arises as to whether the long molecules form the folds in a

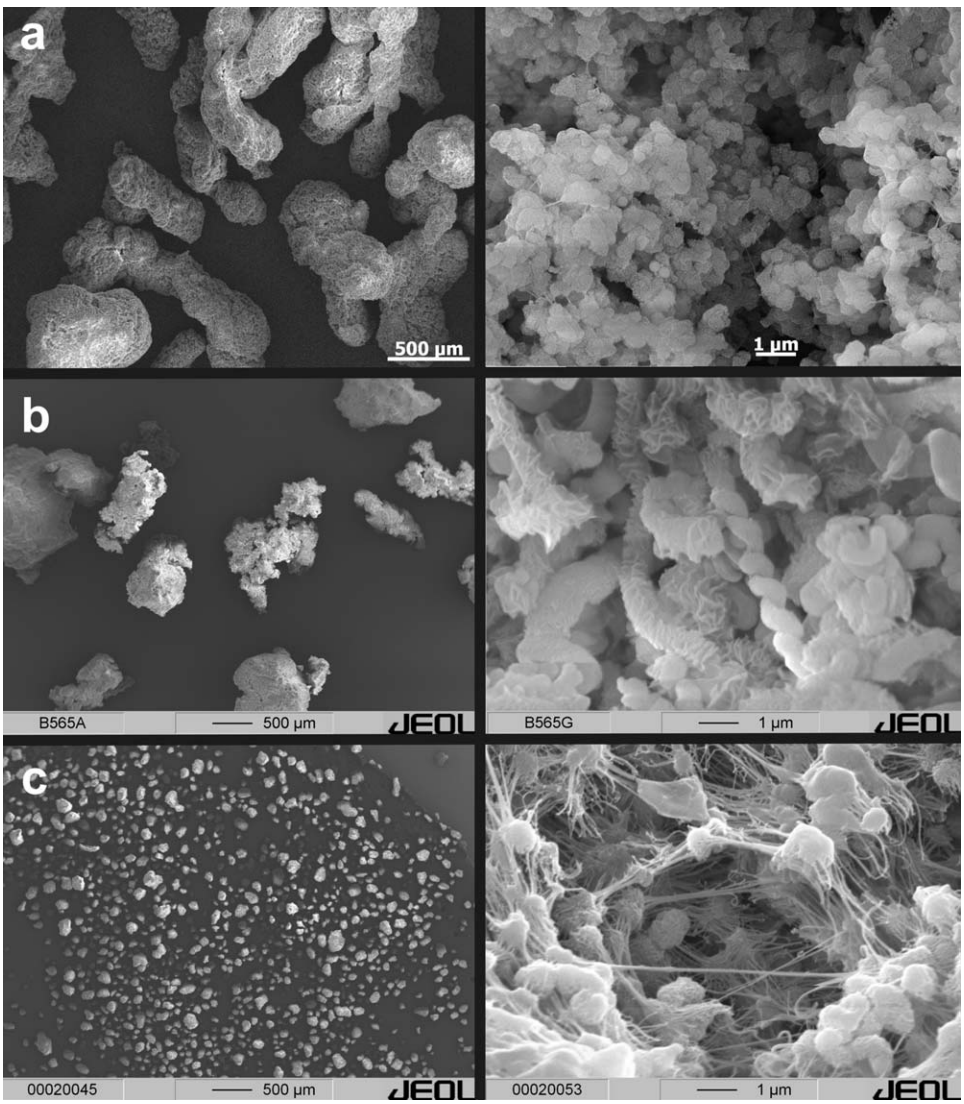

Figure 2 SEM micrographs of typical UHMWPE reactor powders at lower (left) and higher (right) magnifications: broccoli-like M30 powder (A), worm-like B565 powder (B), and cob-web commercial reactor powder (C).

domain or they pass nonfolding from one crystalline domain to another one.

If we consider that the length of an individual molecules of PE with $M_w = 2.5 \times 10^6$ is about 25 μm, and assume that a 3D crystalline domain of the above given size is formed by a regular folded single chain, only 3 μm of a whole molecule would be needed for building this hypothetic domain. Thus, even in this hypothetic case a single molecules should take part in the formation of at least eight crystallites. In fact, the single molecule crosses actually more of them. The domains should be unambiguously connected by tie molecules, which pass from one domain to another. The low contrast between the stained intercrystalline parts (dark) and the nonstained crystalline parts (beads) implies that the difference in density of the crystalline and disordered regions is small. It brings us to assumption that crystalline domains in M30 do not posses a fold-like structure. This assumption is confirmed by sufficiently low free surface energy of crystallites in M30 (24.7 erg/cm^2) calculated on the base of DSC data in[17] as compared with that of a folded-chain single crystal (80 erg/cm^2). However, correctly carrying out DSC measurement[17] gives a modest value of M30 reactor powder crystallinity (65%). It allows us to assume that a portion of macromolecules, growing from small catalytic particles of colloidal size, do form some folds. The crystallites are connected together by the tie molecules, some of them being taut.

The low contrast between the stained and nonstained parts in a section of M30 nascent particle may be caused by various reasons. In particular, the space between neighbor crystalline domains may be too small to seat a marked amount of reduced metallic Ru crystals. If the crystallinity of M30 powder is about 65% and D_{002} is equal 11 nm,[17] the linear

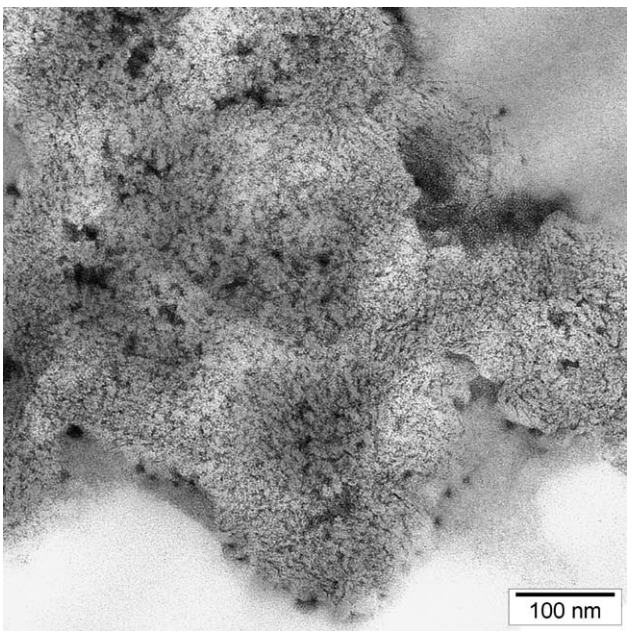

Figure 3 TEM micrographs of a stained section of M30 UHMWPE nascent particles.

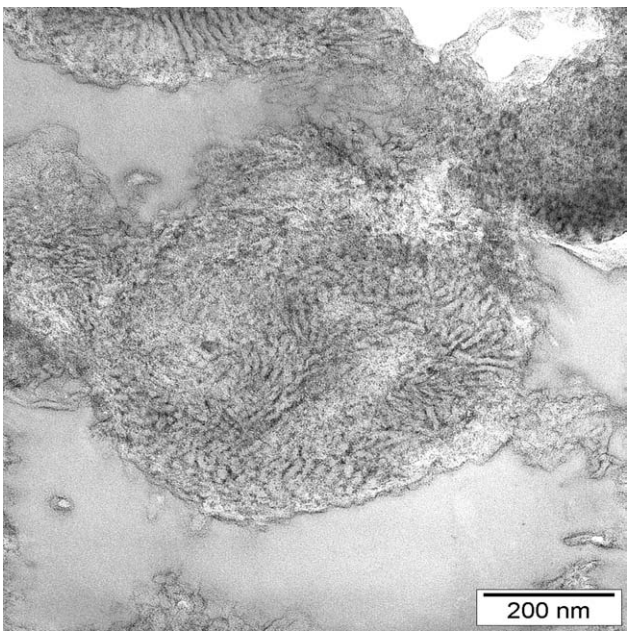

Figure 5 TEM micrograph of a stained section of B565 nascent particle.

dimension of amorphous region should be about 6 nm.

The structure of this space may also influence on the staining. Part of this space is occupied with tie molecules. As distinct from highly entangled molecular segments in the interlamellar space of melt-crystallized PE, the segments of molecules in the nascent M30 do not form the loose loops. The folds (if any) are, probably, tight. The majority of tie molecules are, obviously, in conformation of the perfect trans-zigzag or having small size defects like a $2g_1$kink. The density of intercrystalline regions in M30 powder should be close to that of the crystalline one which hinders their staining by RuO_4.

A large immobile fraction (87.5%) calculated from broadline NMR spectra of M30 powder recorded at room temperature[17] confirms our proposal since the mobility of regular folds and extended tie molecules can be only defreezed when the crystallites begin to melt, so they are represent a so called "rigid

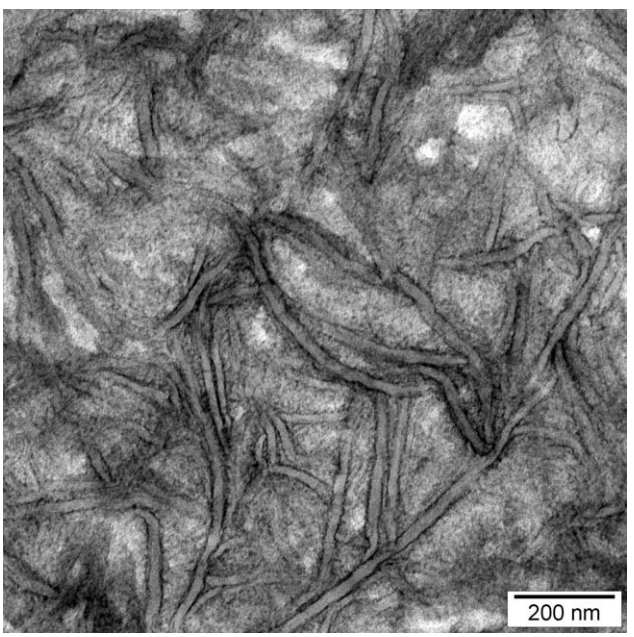

Figure 4 TEM micrograph of a stained section of recrystallized UHMWPE powder.

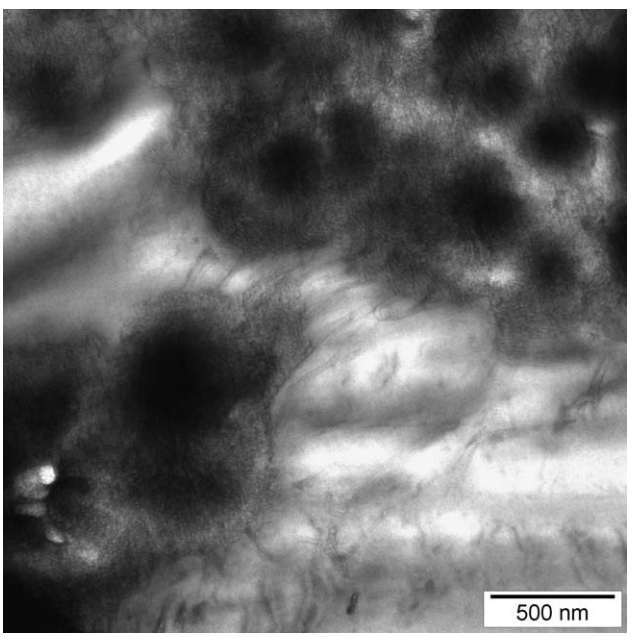

Figure 6 TEM micrograph of a stained section of a commercial powder particle.

TABLE I
Types and Sizes of Morphological Units

Polymer	Individual particle shape	Longitudinal size of individual particles, μm	Transverse size of individual particles, μm	Size of large subparticles, μm	Size of the smallest subparticles, nm	Existence of the fibrils in reactor powders	Fibril diameter nm	Lamella thicknesses nm	Long-periods nm
M18	Broccoli	900–1,700	200–700		150–700	Sporadic	18–34	6.5	12.5
M30	Broccoli	920–1,200	200–700		200–600	Sporadic	18–45	7.5	10.5
M50	Broccoli	700–2,000	200–700		145–570	Sporadic	25–97	7	9.5
M60	Broccoli	450–2,200	200–1,000		120–750	Sporadic	18–60	7	10.5
B565	Irregular shape	880–1,700	280–1,170		Lamellae −18	Spiral worms	530–830	9.5	14
B568	Irregular shape			3–7	50 × 1,000	–		6.5	10
B570	Cob-web	150–1,350	78–800	5–15		Large amount of fibrils between subparticles with lamellae structure	30–100	8.5	14.5
Stamylan	Cob-web spheres	90–440	40–220	8–36	200–700		15–50	7	11

Particle shape, particle size, subparticle size, fibril thickness, type of lamellae, thickness of lamellae, long period of lamellae.

amorphous phase". The existence of this phase explains, in particular, the specific melting of nascent powders observed earlier by the Russian authors.[21] The unusual melting kinetics in polymeric samples having topological constrains is also described in.[22]

After recrystallization, the nascent structure transforms into the classical lamellar one, lamellar thickness depending on crystallization temperature. The growing amount of conformational defects is concentrated in the interlamellar, amorphous regions, increasing the density difference, and, therefore, the staining efficiency and the contrast between crystalline lamellae and amorphous parts (Fig. 4).

The fine structure of lab-scale powder B565 synthesized on a supported heterogeneous Ziegler-Natta catalyst (Fig. 5) differs from that of M30 powder synthesized at nonsupported catalyst particle of colloidal sizes (Fig. 3). The morphological units in Figure 5 seem as the narrow worm-like lamellae. They have, obviously, a mosaic structure because in some of them small beads (crystalline domains) are resolved. As distinct from M30, the crystalline domains in B565 are predominantly united in the lamellae due to a more densely disposition of active centres in the supported catalyst. Since, it is unknown which place of a subparticle has been cut, it is difficult to make a decisive conclusion related to lamella disposition in the spirals, which are characteristics of B565 powder. We may only assume that the lamellae are settled perpendicular to the spiral axis twisting around it because they are oriented in various directions in different parts of the section (Fig. 5). Since the darkening of interlamellar spaces is higher than that in M30 powder one may propose that there are less tight folds, more loose loops and the large number of tie molecules in B565. The smaller amount of adjacent re-entries is confirmed by lower value of surface free energy of crystallite calculated from DSC data (17.5 erg/cm^2)[17] as compared with that in single crystals.

The most complicate situation occurs upon synthesis of commercial UHMWPE grades. First, as it was already discovered in SEM images, coexistence of two types of morphologies is observed in a TEM micrograph of this particle (Fig. 6): spherical-shaped particles and fibrils. It is not a surprise because such kind of structure has been often seen in the reactor powders.[17] The fibrils are considered as the secondary morphological units, comprising the result of catalyst fragmentation because of too fast growing polymeric mass, which is accompanied by plastic deformation of already synthesized polymer.[23,24] The spherical-shaped particles with very dark central parts are well seen in the micrograph. Taking into consideration that the stained section should be a sheet of equal thickness, it is difficult to imagine

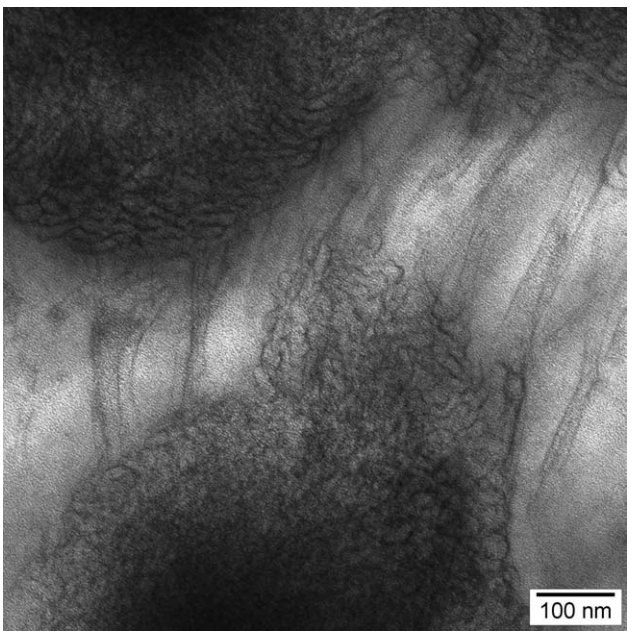

Figure 7 A part of Figure 6 at higher magnification.

that central part of the spherical-shaped units could accumulate much more Ru than the periphery regions. The only reasonable explanation could be as follows: a crack propagates in front of a cutting knife and rounds the individual morphological units because their boundaries are weaker than the inner parts. It results in obtaining a section of uneven thickness and, consequently, an unusual distribution of darkening in a TEM image (Fig. 6).

A question arises as to what is the inner structure of these spherical-shaped, spherulite-like subparticles? The analysis of TEM micrographs presented in Figures 6 and 7 (the latter is snapped at higher magnification) leads us to assumption that the subparticles have different structure in the centre and along the edges. The structural units in the centre seem as the beaded fibrils (or narrow lamellae) while the plate-like lamellae are well resolved on the borders. The revealed difference in the structure may be caused by a change in crystallization conditions of the growing molecules. The polymerisation is the exothermic process. In the beginning of a synthesis in commercial reactors, a catalyst is very active, polymerization rate is high, and the temperature in a vicinity of the catalyst may be higher than melting temperature of PE. The growing molecule begins to crystallize in a far distance from active catalyst site, polymerization rate being higher than crystallization, and formation of plate-like lamellae is more plausible. The polymeric material on periphery is the first, which was synthesized. The primary beaded fibrils (or narrow lamellae) seen in the centre of the subparticles are formed when the polymerization rate slightly slows down, later than the first lamellae crystallized. The secondary fibrils (center of micrograph) are not generating during polymer crystallization. They arise during fragmentation of the catalyst destroying by the fast growing polymeric mass. The secondary fibrils interconnect the small subparticles after the failure of the larger particles. Probably, the catalyst fragments are located in the centre of small subparticles. The character of secondary fibril formation reminds the tensile deformation of PE single crystals when any transition region between the deformed and nondeformed material is observed, and the fibrils are pulling out from lamellae because of unfolding. This implies the unfolding process upon rearrangement of lamellar structure in the fibrillar one.[25]

The surface free energy of crystallites is lower (11 erg/cm^2)[17] than in the powders of M-series, which implies a significant number of tie molecules between crystalline regions and a small amount of regular folds. However, this figure only represent an integral estimate of the surface free energy, which makes it difficult to do any assumption about the molecular packing in disordered regions of secondary fibrils and in subparticles.

Anyway, we see that catalytic system strongly influences on reactor powder morphology on each level of structural organization: from formation of primary fibrils, crystalline domains, lamellae, and nodules to their aggregation in subparticle and the large individual particles.

Morphology of compacted, sintered, and drawn materials

Compacted samples show the same structure than the powder particles (Fig. 8 left) with a clear differentiation between the powder particles, pores as in nascent powders and with only very weak connections between the particles.

Sintering of preliminary compacted films has been performed under the same pressure as it was used at compaction and at a temperature (125°C) several degrees lower than the melting peak. Sintering time was varied from 30 min to 2 h. It was found that reactor powders, which contain fibrillar elements, have a poor compactibility and could not be transformed into monolithic films fit for further drawing under any conditions. The boundaries between the initial individual nascent particles crossing by fibrils remained unchanged—visible both on SEM micrographs of the surface and on micrographs of cryocleaved samples. Reactor powders with a nodular structure (M series and B 568) had the best compactibility and could be transformed into almost transparent films. SEM micrographs demonstrate that the interparticle boundaries have been disappeared. The

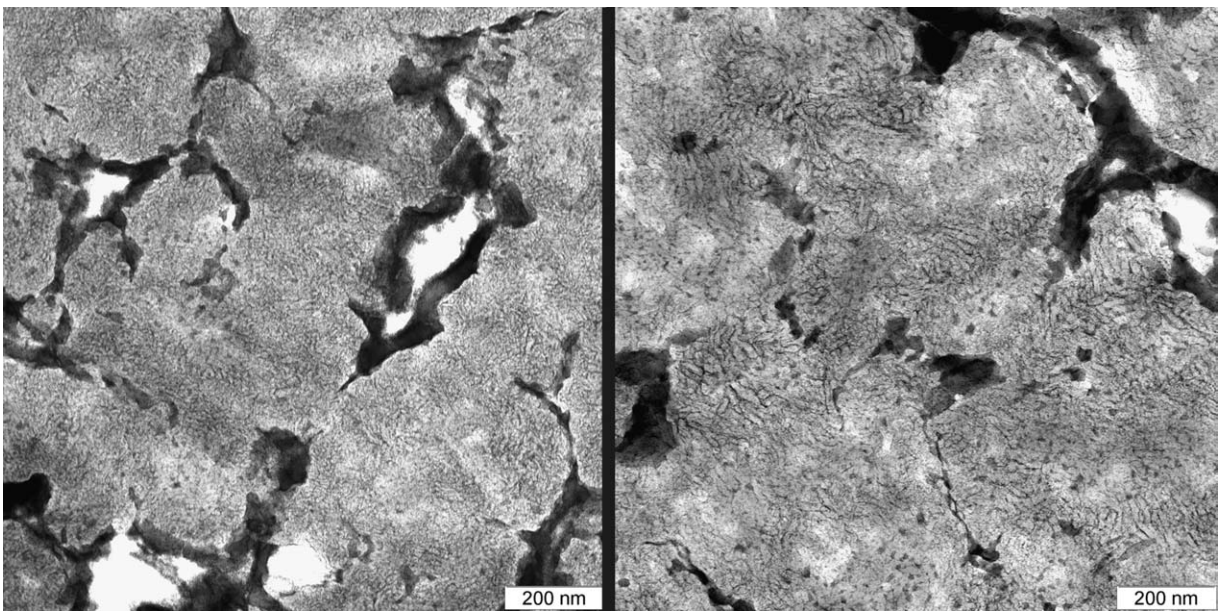

Figure 8 TEM micrograph of stained sections of compacted and sintered films of sample M30 left: after compaction (95 MPa, 10 min) right: after additional sintering (125°C, 95 MPa, 60 min).

particles with the worm-like structure were slightly worse compactable.

Stained ultrathin sections in TEM of all sintered samples revealed a better resolved lamellar structure than in sections of nascent particles, as seen, for example, at the stained sections of compacted and sintered M30 samples (cf Fig. 8 left and right). This increasing difference in staining efficiency and, consequently, in density of crystalline and amorphous regions indicates a better separation between amorphous and crystalline parts. The initial mutual position of the lamellae remains intact in all compacted/sintered powders (for instance, spherical, radial lamellae).

The WAXS study was only carried out for M30 powder demonstrating the best compactability. Both the longitudinal and transverse crystalline sizes increase in the sintered samples, longitudinal size being double. The doubling of longitudinal crystalline size has been observed earlier upon annealing the solution grown lamellae. The possible mechanisms were intensively discussed and the different models of lamellar thickening were proposed. In one of them, a possibility of partial melting preceding the rearrangement of folds is considered,[26] in another one the sliding molecular segments along the crystalline planes are assumed.[27,28] We believe that in this case the former mechanism prevails.

Mechanical properties

The reactor powders with the nodular structure and the best compactibility have been transformed into films with a tensile strength between 3.5 ± 1.7 MPa. Films from particles with worm-like structure had strengths of about 2.1 MPa. Powders having fibrillar elements could be hardly transformed into monolithic films, which were very brittle with a low tensile strength (0.4–0.7 MPa). Influence of pressure during compaction on mechanical properties is illustrated in Figure 9.

Sintering of precompacted films at the enhanced temperature (125°C) results in a pronounced increase of strength. Strength of precompacted/sintered films of powders of the M-series increases by a factor of 6–7, whereas that of precompacted/sintered powders containing the fibrillar elements in the powder particles grows less significant. The maximum strength (32 ± 5 MPa) demonstrates the

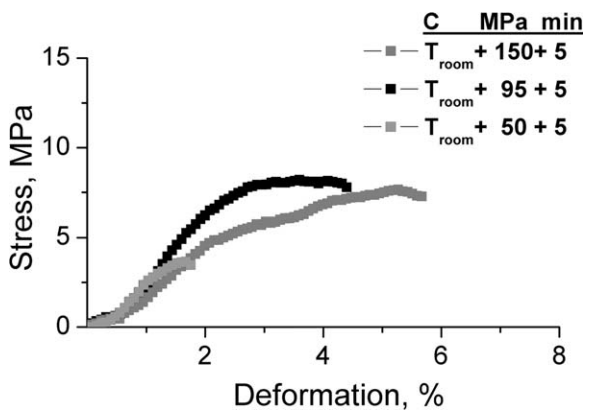

Figure 9 Stress-strain curves of compacted films from reactor powder M30, produced at room temperature and at various pressures for 5 min.

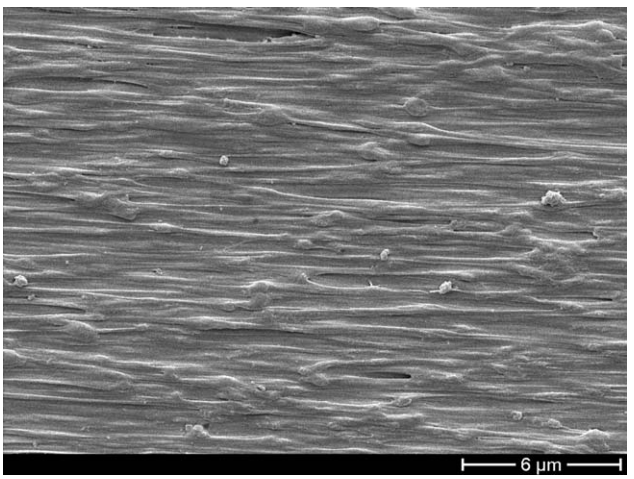

Figure 10 SEM micrograph the surface of the zone-drawn material M30 (draw ratio 14).

compacted/sintered film from M 30 powder, the lowest one (5.6 MPa) was observed for Stamylan. The increase of sintering temperature to 134°C resulted in growing it tensile strength (10 ± 3 MPa) but it remained significantly lower than that of M-films.

But also structural changes of drawn material are expected as shown in a micrograph of the sample surface in Figure 10. The stretched foil of specimen M30 do not show any pores as seen in the compacted material (cf. Fig. 6). The described zone stretching procedure does not only draw the foil, but results also in a homogenisation of the foil. Therefore, one can speak of a healing of the nonperfect compacted foils.

These preliminary results demonstrate the quality of this route of producing films with the high crystallinity of the reactor powders.

CONCLUSIONS

Using different reactor powders of UHMWPE, which have been synthesized with different catalyst systems and under several polymerization conditions, morphology and structure of the powder particles and possibilities to transform the powders into compacted films have been studied. Investigations mainly by means of SEM and TEM revealed details of powder morphology and the semicrystalline structure. The higher crystallinity of the powder particles determined by DSC compared with the lower crystallinity of the material after melting can be explained by a specificity of a structure of interlamellar disordered regions. It is assumed that interlamellar regions of nascent powders contain predominantly tie molecules with low degree of coiling and few amount of folds, while recrystallization after melting results in increase of irregular folds (loose loops) and tie molecules with high degree of coiling. Three types of powder shape and morphology could be defined. It was shown that only powder particles with a nodular structure could be transformed into transparent, strong films by compaction and sintering ("dry technology"). In opposite, powders with complicate lamellar/fibrillar structure have a poor compactibility.

Additional attempts are planned to draw the sintered films to higher draw ratios using a special multistage zone drawing technique developed at the Ioffe Physical Technical Institute.

Practical aim of these studies is opening new possibilities to produce materials of UHMWPE with a high stiffness and a good strength directly from the powder particles. Another aim arises from a better knowledge of conditions to prevent dangerous defects at the boundaries between the powder grains after compaction. Recently, such interparticle defects have been found as the reason for premature damaging of implants in knee joints.

References

1. Smith, P.; Lemstra, P. J. J Mater Sci 1980, 15, 505.
2. Smith, P.; Chanzy, H. D.; Rotzinger, B. P. Polym Comm 1985, 26, 258.
3. Chanzy, H. D.; Rotzinger, B.; Smith, P. US Patent 4,769,433 (1988).
4. Selikhova, V. I.; Zubov, Y. A.; Sinevich, E. L.; Chvalun, S. N.; Ivancheva, N. I.; Smol'yaninova, O. V.; Ivanchev, S. S.; Bakeev, N. E. Vysokomol Soedinen 1992, 34, 92.
5. Kanamoto, T.; Ohama, T.; Tanaka, T.; Takeda, M.; Porter, R. S. Polymer 1987, 28, 1517.
6. Hearle, J. W. S. In High Performance Fibers, Hearle, J. W. S., Ed. Woodhead Publishing Ltd.: Cambridge, 2001, pp 132–150.
7. Afshari, M.; Sikkema, D. J.; Lee, K.; Bogle, M. Polym Rev 2008, 48, 230.
8. Ottani, S.; Ferracini, E.; Ferrero, A.; Malta, V.; Porter, R. S. Macromolecules 1995, 28, 2411.
9. Chanzy, H. D.; Bonjour, E.; Marchessault, R. H. Colloid Polym Sci 1974, 252, 8.
10. Smith, P.; Lemstra, P. J.; Booij, H. C. J Polym Sci: Polym Phys Ed 1981, 19, 877.
11. Frenkel, Y. I. ZhETF 1946, 16, 29.
12. Kuchinski, G. C.; Neuville, B.; Toner, H. P. J Appl Polym Sci 1970, 14, 2069.
13. Aulov, V. A.; Makarov, S. V.; Kuchkina, I. O.; Pantyukhin, A. A.; Ozerin, A. N.; Bakeev, N. F. Vysokomol Soedinen 2002, 44, 1367.
14. Siegman, A.; Raiter, I.; Narkis, M.; Eyrer, P. J Mater Sci 1986, 21, 1180.
15. Han, K. S.; Wallace, J. F.; Truss, R. W.; Geil, P. H. Polym Eng Sci 1980, 20, 747.
16. Aulov, V. A.; Makarov, S. V.; Kuchkina, I. O.; Ozerin, A. N.; Bakeev, N. F. Polym Sci 2000, 42, 1190.
17. Myasnikova, L. P.; Boiko, Y. M.; Ivan'kova, E. M.; Egorov, V. M.; Lebedev, D. V.; Marikhin, V. A.; Radovanova, E. I.; Michler, G. H.; Seydewitz, V.; Goerlitz, S. In Reactor Powder

Morphology, Myasnikova, L. P., Lemstra, P., Eds. NOVA Science Publisher: Hauppauge, NY.
18. Uehara, H.; Nakae, M.; Kanamoto, T.; Ohtsu, O.; Sano, A.; Matsuura, K. Polymer 1998, 39, 6127.
19. Uehara, H.; Uehara, A.; Kakiage, M.; Takahashi, H.; Murakami, S.; Yamanobe, T.; Komoto, T. Polymer 2007, 48, 4547.
20. Michler, G. H. Electron Microscopy of Polymers; Springer: Berlin, 2008.
21. Egorov, V. M.; Ivan'kova, E. M.; Marikhin, V. A.; Myasnikova, L. P.; Baulin, A. A. Polym Sci Ser A 1999, 41, 1131.
22. Lippits, D. R.; Rastogi, S.; Hoehne, G. W. H. Phys Rev Lett 2006, 96, 218303.
23. Munoz-Eskalona, A.; Villamizar, C.; Frias, R. Polym Sci Tech (Struct-Property Relat Polym Solids) 1983, 22, 95.
24. Chanzy, H. D.; Revol, J. F.; Marchessault, R. H.; Lamande, A. Kolloid Z Z Polym 1973, 25, 563.
25. Marikhin, V. A.; Myasnikova, L. P. Oriented Polymer Materials, Fakirov, S., Ed. Huethig &Wepf: Mainz, 1996; Chapter 2, pp 36–92.
26. Wunderlich, B. Macromolecular Physics; Academic Press: New York, 1976; Volume 2.
27. Cheng, S. Z. D.; Zhu, L.; Li, C. Y.; Honigfort, P. S.; Keller, A. Thermochim Acta 1999, 32, 105.
28. Rastogi, S.; Terry, A. E. Adv Mater 2005, 180, 161.